Official journal website:
amphibian-reptile-conservation.org

Amphibian & Reptile Conservation
19(2): 59–69 (e350.1).

Multi-Scale Synergistic Optimization and Life Cycle Assessment of Blue-Green Infrastructure for Addressing Agricultural Non-Point Source Pollution and Conserving Amphibian Habitats

[1]DENG Wen-jia

[1]*Xi'an Mingde Institute of Technology, Xi'an 710124, China*

***Abstract.*— Agricultural intensification has increased non-point source pollution and degraded freshwater habitats essential for amphibian survival and reproduction. Existing control strategies generally focus on local pollution reduction while overlooking habitat connectivity and the life-cycle carbon footprint of blue–green infrastructure. This study examines a typical intensive agricultural watershed in the middle and lower reaches of the Yangtze River and develops an integrated framework combining spatial optimization, carbon accounting, and amphibian habitat conservation. The SWAT model is used to simulate watershed pollution processes and identify critical source areas and transport pathways affecting wetlands, riparian zones, and potential amphibian breeding habitats. The NSGA-II algorithm is then applied to optimize the spatial configuration of blue–green infrastructure across fields, drainage ditches, and river corridors. Life-cycle assessment is employed to quantify pollution-reduction efficiency, carbon footprint, and implementation cost. The optimized configurations reduce total nitrogen and total phosphorus loads by 15.8%–19.1% and 20.5%–23.1%, respectively, while maintaining a comparatively low net carbon footprint. Improved nutrient interception and the restoration of connected wetland and riparian features can reduce environmental pressures on amphibian breeding and dispersal habitats. These findings demonstrate the potential of multi-scale blue–green infrastructure to coordinate agricultural pollution control, low-carbon watershed management, and amphibian habitat conservation.**

Keywords. Agricultural Non-Point Source Pollution, Blue-Green Infrastructure, Multi-Scale Collaborative Optimization, Life Cycle Assessment

Citation: Wen-jia D. 2025. Multi-Scale Synergistic Optimization and Life Cycle Assessment of Blue-Green Infrastructure for Addressing Agricultural Non-Point Source Pollution. *Amphibian & Reptile Conservation* 19(2): 59–69 (e350.1).

Accepted: 25 July 2025; **Published:** 19 December 2025

Introduction

Agricultural intensification has substantially increased food production, but it has also transformed freshwater and terrestrial ecosystems through excessive fertilizer application, pesticide use, soil disturbance, drainage modification, and the removal of natural vegetation. These activities generate agricultural non-point source pollution that is transported through surface runoff, subsurface flow, drainage ditches, and river networks. Unlike pollution from identifiable point sources, agricultural runoff originates from spatially dispersed activities and varies according to land use, rainfall, soil properties, crop-management practices, and watershed hydrology. Its diffuse and dynamic nature makes it particularly difficult to monitor and control. In intensive agricultural watersheds, elevated concentrations of nitrogen, phosphorus, suspended sediment, pesticides, and other contaminants can degrade water quality and threaten organisms that depend on interconnected freshwater and terrestrial habitats.

Amphibians are among the biological groups most vulnerable to these environmental changes. Their permeable skin, aquatic or semi-aquatic reproductive

Correspondence. **dwwwjjj163@163.com*

stages, limited dispersal capacity, and dependence on both terrestrial and freshwater environments expose them to contaminants throughout multiple phases of their life cycles. Agricultural pollutants may enter amphibian habitats through runoff into ponds, wetlands, irrigation channels, drainage ditches, riparian areas, and slow-flowing river sections. Nutrient enrichment can promote eutrophication, alter dissolved oxygen concentrations, modify aquatic vegetation, and disrupt food-web structure. Sediment deposition may reduce the availability and quality of breeding sites, while pesticides and other agrochemicals can affect amphibian survival, development, behavior, reproduction, and immune function. Even when contaminant concentrations are not immediately lethal, prolonged or repeated exposure may produce sublethal effects that reduce population viability.

The conservation implications extend beyond water-quality deterioration. Intensive agricultural development frequently causes the drainage or fragmentation of wetlands, simplification of riverbanks, removal of vegetated field margins, and conversion of natural dispersal corridors. As a result, amphibian populations may become isolated within small and degraded habitat patches. Such isolation can restrict seasonal movement between breeding and terrestrial habitats, reduce opportunities for recolonization, and increase vulnerability to local extinction. Climate change may intensify these pressures by altering precipitation patterns, increasing drought frequency, and producing more extreme runoff events. Effective amphibian conservation in agricultural landscapes must therefore address not only contaminant loads but also habitat availability, hydrological stability, landscape connectivity, and the long-term environmental consequences of management interventions.

Blue–green infrastructure offers a potentially valuable approach to addressing these interconnected challenges. It includes natural and semi-natural landscape features designed to manage water, nutrients, sediments, and ecological processes. In agricultural watersheds, relevant measures may include constructed wetlands, retention ponds, vegetated buffer strips, restored riparian corridors, grassed waterways, ecological drainage ditches, field margins, and floodplain restoration. These features can intercept runoff, retain sediments, remove nutrients, moderate peak flows, and improve watershed resilience. When appropriately designed and located, they may also create or restore amphibian breeding areas, terrestrial refuges, foraging grounds, and movement corridors.

The ecological value of blue–green infrastructure, however, cannot be assumed solely from its pollution-removal performance. A structure designed primarily for water treatment may not necessarily provide suitable amphibian habitat. For example, steep-sided retention basins, permanent ponds dominated by predatory fish, highly disturbed drainage channels, or wetlands with unsuitable hydroperiods may offer limited conservation benefits. Conversely, shallow vegetated ponds, seasonally inundated wetlands, connected riparian buffers, and pesticide-free terrestrial margins may support breeding, larval development, shelter, and dispersal. Infrastructure planning must therefore consider habitat quality, hydroperiod, vegetation structure, connectivity, contaminant exposure, and the ecological requirements of amphibian species alongside conventional engineering indicators.

Most existing agricultural pollution-control strategies remain concentrated at individual fields or isolated river sections. Such localized interventions may reduce pollution at specific points but fail to account for pollutant generation, transport, accumulation, and ecological exposure across the entire watershed. They may also overlook the spatial relationships between amphibian breeding habitats and the surrounding terrestrial landscape. A measure located in a hydrologically important pollution pathway may deliver substantial water-quality benefits, whereas another intervention may be more valuable for connecting fragmented amphibian habitats. Optimizing only one scale or objective can consequently produce an inefficient distribution of resources and may create trade-offs between pollution control, habitat conservation, cost, and greenhouse-gas emissions.

A multi-scale framework is required to coordinate interventions across fields, drainage ditches, wetlands, riparian corridors, and river systems. At the field scale, vegetated margins and runoff-control measures can reduce the initial mobilization of nutrients, sediments, and agrochemicals while providing terrestrial refuge. At the ditch scale, ecological channels and treatment wetlands can intercept pollutants and function as movement pathways. At the riparian and river scales, restored vegetation and floodplain habitats can improve water quality, stabilize banks, and enhance connectivity among aquatic and terrestrial habitat patches. Coordinating these measures can generate cumulative benefits that are unlikely to be achieved through isolated projects.

The implementation of blue–green infrastructure may nevertheless involve environmental costs. Construction materials, excavation, transportation, maintenance, vegetation management, and eventual rehabilitation can generate greenhouse-gas emissions. Wetlands and retention systems may also produce methane or nitrous oxide under particular hydrological and biogeochemical conditions. Assessing only operational pollution reduction could therefore overestimate the overall sustainability of an intervention. Life cycle assessment provides a systematic method for quantifying carbon emissions and other environmental burdens from construction through operation, maintenance, and end-of-life management. Integrating life cycle assessment with ecological conservation is especially important because climate change itself represents a major threat to amphibian populations through habitat drying, altered breeding seasons, extreme temperatures, and changing disease dynamics.

Spatially explicit watershed modelling and multi-objective optimization provide the technical foundation for such integration. The Soil and Water Assessment Tool can simulate hydrological processes and estimate the generation and transport of nutrients and sediments under different land-use and management conditions. Its outputs can help identify critical source areas and migration pathways that contribute disproportionately to downstream pollution and amphibian habitat degradation. The Non-dominated Sorting Genetic Algorithm II can then evaluate alternative blue–green infrastructure configurations while balancing multiple and potentially competing objectives, including nutrient reduction, implementation cost, life-cycle carbon footprint, and amphibian habitat conservation.

Within this framework, amphibian conservation should be represented through spatially relevant indicators rather than treated as an incidental benefit of improved water quality. Potential indicators include the protection and restoration of breeding wetlands, water-quality improvement within reproductive habitats, suitable hydroperiods, vegetated buffer coverage, distances between aquatic and terrestrial habitats, and connectivity among habitat patches. Incorporating these considerations makes it possible to identify configurations that intercept pollutants while also strengthening the ecological functions required by amphibians throughout their life cycles. Accordingly, this study develops an integrated framework combining watershed pollution simulation, multi-scale spatial optimization, life cycle assessment, and amphibian habitat-conservation considerations in an intensive agricultural watershed in the middle and lower reaches of the Yangtze River. The study aims to: (1) identify critical agricultural pollution-source areas and transport pathways that may affect amphibian habitats; (2) optimize the distribution of blue–green infrastructure across field, ditch, riparian, and river scales; (3) evaluate the performance of alternative configurations in reducing total nitrogen and total phosphorus loads; (4) assess their costs and life-cycle carbon footprints; and (5) examine how pollution-control measures can improve habitat quality and connectivity for amphibians. By integrating engineering, climatic, and ecological objectives, the study seeks to provide a decision-support framework for agricultural watershed management that contributes simultaneously to water-quality improvement, carbon-conscious infrastructure planning, and amphibian conservation.

Related Work

With the acceleration of agricultural intensification, agricultural non-point source pollution has become a key challenge for global water environment governance. The control of agricultural non-point source pollution increasingly emphasizes multi-party cooperation and co-production models. Vetter (2022) revealed the complex reality of cooperative governance in agricultural non-point source pollution control. Tanık et al. (2021) identified the main pollution hotspots and pollutants by analyzing land use, agricultural production methods, and water quality conditions within the watershed. Plunge et al. (2023) constructed a cost assessment model to quantitatively analyze the emission reduction effects and costs of different agricultural non-point source pollution control scenarios. Tanner et al. (2025) selected and designed matching interception measures based on their understanding of pollutant migration pathways (source flow sink), taking into account hydrological processes, land characteristics, and pollutant types. Rojas-Rodríguez et al. (2021) used hydrological and water quality modeling methods to simulate agricultural non-point source pollution in the watershed.

In the intensive agricultural areas of southern Bulgaria, a large amount of fertilizers, pesticides, etc., are used and enter the groundwater system through leakage and runoff, leading to deterioration of groundwater quality and significant agricultural non-point source pollution. Simeonova (2024) combined land use data and statistical analysis methods to analyze the sources of groundwater pollution in the study area. Krivtsov (2025) provides an overview of the various ecosystem services offered by blue-green infrastructure. LIU et al. (2025) summarized the mechanisms of urban blue-green infrastructure for enhancing carbon sequestration and reducing carbon emissions. Yan et al. (2025) used Anyang City as the research area, based on the theory of blue-green infrastructure, and applied geographic information systems and MIKE FLOOD model to construct a water ecological security pattern. Guo et al. (2024) studied the relationship between landscape pattern and function of blue-green infrastructure. There have been significant advances in the identification, simulation, and management strategies of agricultural non-point source pollution in existing research, but there are still obvious limitations: on the one hand, most studies focus on single technology or local scale analysis, and fail to fully integrate multi-scale spatial collaboration; On the other hand, the planning of blue-green infrastructure often focuses on hydrological or ecological functions, lacking a systematic assessment of its full lifecycle carbon footprint, which may overlook its comprehensive benefits and potential trade-offs under carbon neutrality goals. Therefore, this article constructs an integrated analysis framework combining spatial intervention and carbon accounting to compensate for the shortcomings of existing research in system collaboration and quantification of environmental impacts throughout the lifecycle, thus providing scientific basis for governance paths towards sustainable agriculture and water security.

Method

Overview of the Research Area and Data Foundation

This study selected a typical intensive agricultural small watershed located in the middle and lower reaches of the Yangtze River as the case area, with a watershed area of approximately 85 square kilometers. The region has a subtropical monsoon climate with an average annual rainfall of 1250 millimeters. The land use is mainly paddy fields and dry land, and the distribution of land use types is shown in Table 1 (Hamel and Tan, 2022; Mugume and Nakyanzi, 2024):

Table 1: Distribution of Land Use Types in the Study Area.

Land Use Type	Area (hectares)	Proportion (%)	Main Crop/Function
Paddy Field	5950	70.0	Rice
Dryland	1700	20.0	Wheat
Woodland	420	5.0	Ecological Conservation
Construction Land	310	3.6	Residential Areas
Water Body	120	1.4	Rivers and Ditches

The watershed water system is a three-level ditch network that flows into a main river channel. The basic geographic data uses a 1:10000 digital elevation model to generate watershed boundaries, river networks, and sub watershed divisions. The land use data is derived from annual land use remote sensing interpretation maps.

The soil data is based on a 1:50000 soil map and combined with field sampling to determine key physical and chemical parameters, including soil texture, organic carbon content, and effective field capacity, as shown in Table 2:

Table 2: Soil Parameters.

Soil Type	Organic Carbon Content (g/kg)	Available Field Capacity (mm)	Texture Type
Red Soil	12.8	120	Clay Loam
Paddy Soil	18.5	180	Loam
Yellow-brown Earth	9.6	90	Sandy Loam
Fluvo-aquic Soil	7.2	60	Clay
Vegetable Garden Soil	15.3	150	Loamy

The meteorological driving data comes from daily scale data from three national meteorological stations within and around the basin, including precipitation, maximum and minimum temperatures, wind speed, relative humidity, and solar radiation. The hydrological and water quality data adopts the daily flow monitoring data of the hydrological station at the outlet of the basin for three consecutive years and the water quality sampling data at least once a month (including total nitrogen, total phosphorus, nitrate nitrogen, and ammonia nitrogen concentrations), which are used for model calibration and verification. Agricultural production management data, such as crop rotation systems, fertilization dates, fertilization amounts, and irrigation arrangements, are obtained through a combination of farmer surveys and local agricultural statistical yearbooks (Breulmann et al., 2024; Willems et al., 2023).

Simulation of Non-Point Source Pollution Process and Source Sink Analysis in the Watershed

This article uses the SWAT2012 model to construct a model for studying distributed hydrology and non-point source pollution processes in watersheds. Firstly, based on a 10-meter resolution DEM and actual river network data, a minimum watershed area threshold of 50 hectares is set to divide the entire watershed into 42 sub watersheds.

Secondly, by overlaying land use and soil type maps, a 5% area threshold is set for 587 hydrological response units (Ariyarathna et al., 2023; Sadegh Koohestani et al., 2025). The meteorological, soil, vegetation, and management databases required for the model are constructed based on the data from the previous section. The calibration and validation of key model parameters are carried out using the SUFI-2 algorithm in SWAT-CUP, which iteratively adjusts the parameter set to maximize the degree of agreement between observed and simulated values.

Its objective function is usually defined as the weighted form of the sum of squared residuals between observed and simulated values.

$$\phi(\theta)=\sum_{t=1}^{N}\left[w_t\cdot(Q_{obs,t}-Q_{sim,t}(\theta))^2\right] \tag{1}$$

θ is the parameter vector to be calibrated, $Q_{obs,t}$ and $Q_{sim,t}$ are the observed and simulated runoff (or pollutant load) at time t, w_t is the weight coefficient, and N is the length of the time series. This optimization process improves simulation reliability by continuously narrowing the parameter uncertainty interval.

Calibrate and validate the simulation results of monthly runoff, total nitrogen, and total phosphorus loads using Nash efficiency coefficient (NSE) and determination coefficient (R^2) as the main evaluation indicators (Figure 1) (Willems et al., 2021). NSE is used to quantify the goodness of fit between simulated and observed sequences, and its calculation formula is as follows:

$$NSE=1-\frac{\sum_{t=1}^{N}(Q_{obs,t}-Q_{sim,t})^2}{\sum_{t=1}^{N}(Q_{obs,t}-\bar{Q}_{obs})^2} \quad (2)$$

$\bar{Q}_{obs}$ is the average of observed values. The closer NSE is to 1, the better the simulation effect.

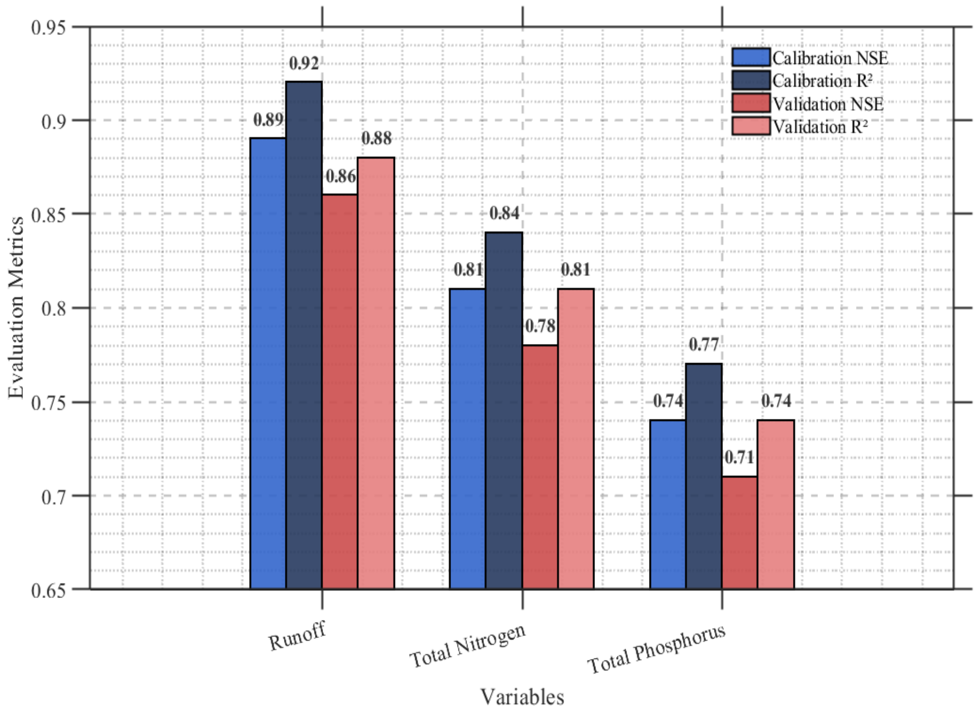

Fig. 1. Model Calibration and Validation Results.

The NSE and R^2 of runoff simulation reached 0.89 and 0.92 (calibration period), 0.86 and 0.88 (validation period), respectively, indicating that the model has excellent simulation accuracy and reliability.

Sensitivity analysis identifies the parameters most sensitive to runoff and pollutant loads, including the number of runoff curves (CN2), soil evaporation compensation coefficient (ESCO), groundwater delay time (GW_DELAY), nitrogen and phosphorus application efficiency, etc. (Konstantinova et al., 2024; Winker et al., 2022).

After completing the model calibration verification, run the benchmark scenario simulation and output the spatial distribution map of the annual average total nitrogen and total phosphorus load intensity of each hydrological response unit in the watershed. By analyzing the superposition of load intensity and hydrological path, high load areas that contribute about 70% of the total load of the watershed are identified as key source areas, and the main transport channels for pollutants from fields to rivers through ditches are clarified. Among them, the migration and transformation process of pollutants in rivers can be described by a first-order kinetic equation, for example, the decay of total phosphorus in rivers is:

$$\frac{dC}{dt}=-k_{TP}\cdot C \quad (3)$$

C is the total phosphorus concentration, and k_{TP} is the decay rate constant of total phosphorus. This relationship helps to understand the natural reduction effect of pollutants during transport.

Multi-scale Blue-Green Infrastructure Collaborative Optimization Model

Optimize the model to deploy three types of blue-green infrastructure on identified pollution sources and migration paths.

The decision variables at the field scale are the placement and length of ecological interception ditches and vegetation buffer zones, and their optional locations are limited to the downstream edge of key source area farmland or adjacent drainage ditches. The decision variables for the scale of the ditch are the construction location and treatment area of the multi-pond wetland system, and the optional locations are the catchment nodes and flow velocity reduction zones of each level of ditch.

The decision variables at the river scale are the implementation river section and width of the riverbank vegetation ecological restoration project (Peters and Landström, 2022; Yonegura, 2025).

This optimization model aims to achieve the dual goals of environment and economy in synergy, and its multi-objective optimization problem can be formally expressed as:

$$\begin{array}{ll} \text{Maximize} & f_1(X)=(\eta_{TN}(X),\eta_{TP}(X)) \\ \text{Minimize} & f_2(X)=A_{total}(X) \end{array} \tag{4}$$

X refers to the set of all decision variables, that is, the layout plan of each facility; $f_1(X)$ is the environmental objective, which is the vector of the total nitrogen and total phosphorus load reduction rates η_{TN} and η_{TP} at the outlet of the watershed, integrated into the comprehensive pollution load reduction rate; $f_2(X)$ is the economic target, which refers to the total land area $A_{total}$of all facilities.

The optimization process needs to meet a series of spatial constraints, including: facilities must not occupy basic farmland, the upper limit of single facility area, and the minimum distance between facilities of different scales to avoid functional overlap. These constraints can be uniformly expressed as:

$$G_i(X)\leq 0,g=1,2,...,m \tag{5}$$

$G_i(X)$ is the i-th constraint function, and m is the total number of constraints. The model ensures that all generated solutions are spatially feasible through constraint handling mechanisms.

Adopting the Non-Dominated Sorting Genetic Algorithm with Elite Strategy (NSGA-II) for multi-objective optimization solution. The algorithm parameters are set as follows: population size of 100, maximum number of evolutionary generations of 200, crossover probability of 0.9, and mutation probability of 0.1.

The core of this algorithm lies in guiding population evolution through non dominated sorting and crowding degree calculation. Its individual selection mechanism depends on the dominance relationship, that is, for any two solutions X_1 and X_2, if:

$$\begin{cases} \forall j\in\{1,2\}10,f_j(X_1)\geq f_j(X_2) \\ \exists k\in\{1,2\},f_k(X_1)>f_k(X_2) \end{cases} \tag{6}$$

For the maximization objective, it is called X_1 dominating X_2. Through iterative evolution, a set of non dominated solutions is finally obtained, forming a Pareto optimal frontier. Each solution corresponds to a specific set of infrastructure spatial layout schemes, providing decision-makers with multiple optimal choices to balance pollution reduction efficiency and land use costs (Mueca et al., 2025; O'Donnell et al., 2021).

Whole Life Cycle Carbon Footprint and Cost Assessment

For each optimization plan, calculate its full lifecycle carbon footprint and cost. The system boundary covers four stages: building material production, on-site construction, 20-year operation and maintenance, and demolition and recycling. Carbon emission accounting adopts process analysis method and emission factor method.

Table 3 shows the key parameters for assessing the full lifecycle carbon footprint and cost:

Table 3: Key Parameters for Life Cycle Carbon Footprint and Cost Assessment

Parameter Category	Parameter Name	Unit	Reference Value
Emission Factors for Material Production	Emission factor for concrete production	kg CO_2-eq/m³	280
	Emission factor for steel production	kg CO_2-eq/kg	2.15
	Emission factor for aggregate production	kg CO_2-eq/ton	2.8
Carbon Sequestration Parameters for O&M	Annual biomass growth rate of wetland vegetation	ton DM/(ha·yr)	8.5
	Annual biomass growth rate of buffer strip shrubs	ton DM/(ha·yr)	4.2
	Carbon fraction of biomass	dimensionless	0.47
	Carbon retention coefficient	dimensionless	0.75

In the production stage of building materials, the upstream production energy consumption and process emissions of major building materials such as concrete, steel, sand and gravel are mainly accounted for, and the data is sourced from the China Life Cycle Basic Database.

The carbon emissions at this stage can be calculated based on consumption and emission factors:

$$C_{material}=\sum_r (Q_{m,r}\times EF_{m,r}) \tag{7}$$

$C_{material}$ refers to the total carbon emissions during the production stage of building materials, where $Q_{m,r}$ is the consumption of the r-th type of building material, and $EF_{m,r}$ is the unit production emission factor corresponding to the building material.

During the construction and demolition phases, calculate the diesel consumption of mechanical equipment and the direct emissions generated by earthwork operations.

During the operation and maintenance phase, calculate the energy consumption of facility pumping (if any), the emissions generated from regular harvesting and disposal of plants, and measure the annual biomass carbon sequestration of the vegetation system using the IPCC recommended carbon sink calculation method. The carbon sink increment can be estimated using the following formula:

$$\Delta C_{seq}=\sum_{t=1}^{T} (G_t\times CF\times(1-R)) \tag{8}$$

ΔC_{seq} is the total carbon sink increment during the accounting period, G_t is the annual biomass growth in year t, CF is the biomass carbon content, R is the retention coefficient considering factors such as litter decomposition, and T is the operating period.

Cost analysis includes one-time investments in materials, labor, and machinery during the construction period, as well as annual costs such as maintenance, management, and energy consumption during the operation period, discounted to net present value over a 20-year period. The formula for calculating net present value is:

$$NPV=C_0+\sum_{t=1}^{T}\frac{C_t}{(1+l)^t} \quad (9)$$

NPV is the net present value of total cost, C_0 is the initial construction investment, C_t is the operating and maintenance cost in year t, and l is the discount rate.

All greenhouse gas emissions are uniformly converted into carbon dioxide equivalents, and the net carbon footprint (total carbon emissions minus carbon sink increment) and carbon footprint intensity corresponding to the reduction of unit pollution load for each scheme are finally calculated.

The calculation method for this intensity index (CI) is as follows:

$$CI=\frac{C_{net}}{\Delta L} \quad (10)$$

C_{net} is the net carbon footprint of the scheme, and ΔL is the total nitrogen or total phosphorus load reduction achieved by the scheme throughout its entire lifecycle. This intensity index effectively measures the comprehensive efficiency of different pollution control schemes between environmental benefits and climate impacts.

Results and Discussion

Spatial Distribution Characteristics of Non-Point Source Pollution in the Watershed

There is significant spatial heterogeneity in the annual average TN and TP load intensity of each sub basin. The TN load intensity range is between 5.2 and 32.7 kg/ha·yr, and the TP load intensity range is between 0.8 and 5.4 kg/ha·yr. The high load areas are concentrated in the relatively flat terrain, contiguous farmland, and areas with high fertilization intensity in the central and northern parts of the basin. The spatial distribution heatmap (Figure 2) intuitively illustrates the cumulative effect of pollution load transport from upstream to downstream and from key source areas to river channels, providing spatial targeting for the precise deployment of blue-green infrastructure in the future.

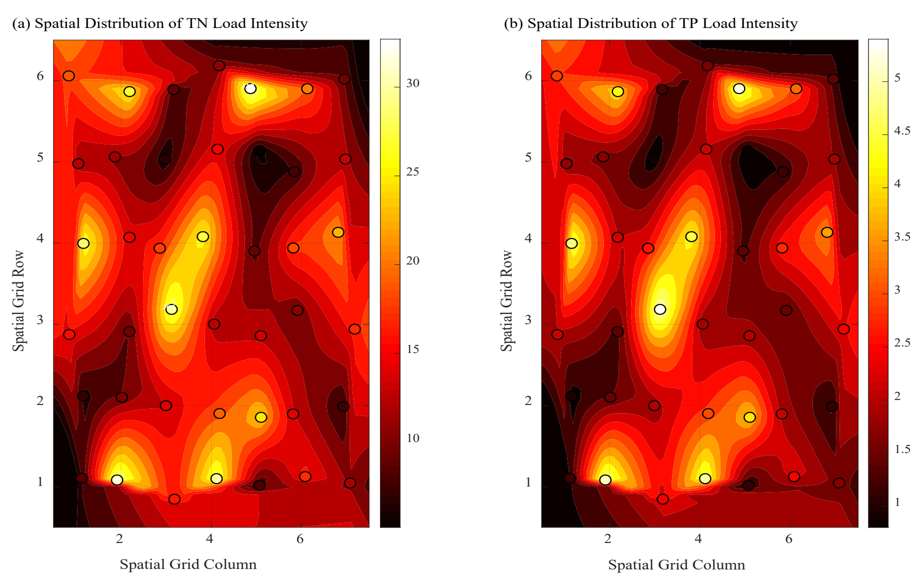

Fig. 2. Distribution of Pollution Space

The visualization results intuitively confirm the spatial heterogeneity and highly concentrated characteristics of pollution load within the watershed, providing a direct spatial basis for the differentiated and precise layout of multi-scale blue-green infrastructure in the future.

Comparison of Optimization Layout Plans for Blue Green Infrastructure

After completing the NSGA-II algorithm solution, this paper selects the scheme with the best comprehensive performance from the Pareto front as the "collaborative optimization scheme". At the same time, based on the total area of the watershed and the total length of the ditch, facilities of the same type are arranged according to the principle of uniform spacing, forming a "traditional homogenization scheme".

Using the SWAT model to simulate the hydrological and water quality processes after the implementation of two schemes, the quantity, total land area, and spatial distribution density of each facility in the two schemes were counted and summarized, and Table 4 comparative analysis data was obtained:

Table 4: Blue and Green Infrastructure Configuration for Different Layout Plans

Facility Type	No. in Conventional Scheme	No. in Optimized Scheme	Total Area in Conventional Scheme (ha)	Total Area in Optimized Scheme (ha)
Vegetated Swale	18	22	5.4	4.8
Vegetated Buffer Strip	15	11	9.0	6.2
Multi-pond Wetland System	7	5	3.5	2.5
Riparian Ecological Restoration	12	9	14.4	10.8
Total	52	47	32.3	24.3

The collaborative optimization scheme achieves more intensive land use by precise spatial targeted layout, with fewer facilities and total land area than traditional schemes.

Although the number of ecological interception ditches in the optimization plan has slightly increased to strengthen the source interception of runoff in key source areas, their unit length efficiency is higher, resulting in a decrease in the total area. At the same time, the optimization plan significantly reduced the number and area of large-scale facilities such as vegetation buffer zones, multi-pond wetlands, and riverbank restoration, indicating that its layout is more focused on key nodes along the pollutant migration path rather than uniform distribution.

Pollution Reduction Results

Taking a continuous 5-year simulation period as the evaluation period, this article compares and analyzes the differences in pollutant interception efficiency between two layout strategies by calculating the pollution load reduction rates of each scheme relative to the baseline scenario. The model runs using a calibrated parameter set, and meteorological driven data uses contemporaneous observation sequences to ensure the comparability and reproducibility of simulation results. The specific reduction rate results are shown in Figures 3 and 4:

The TN reduction rate of the collaborative optimization scheme has remained consistently higher than that of the traditional scheme over the past five years, with a fluctuation range of 15.8% -19.1%, while the traditional scheme ranges from 12.5% -15.0%. This indicates that multi-scale collaborative optimization not only improves the absolute efficiency of pollution reduction, but more importantly, establishes a more resilient pollution interception system. It effectively buffers the impact of interannual hydrological fluctuations through precise spatial matching of "source process end", providing a quantifiable and replicable technical path and decision-making basis for achieving the long-term and stable management of the agricultural non-point source pollution.

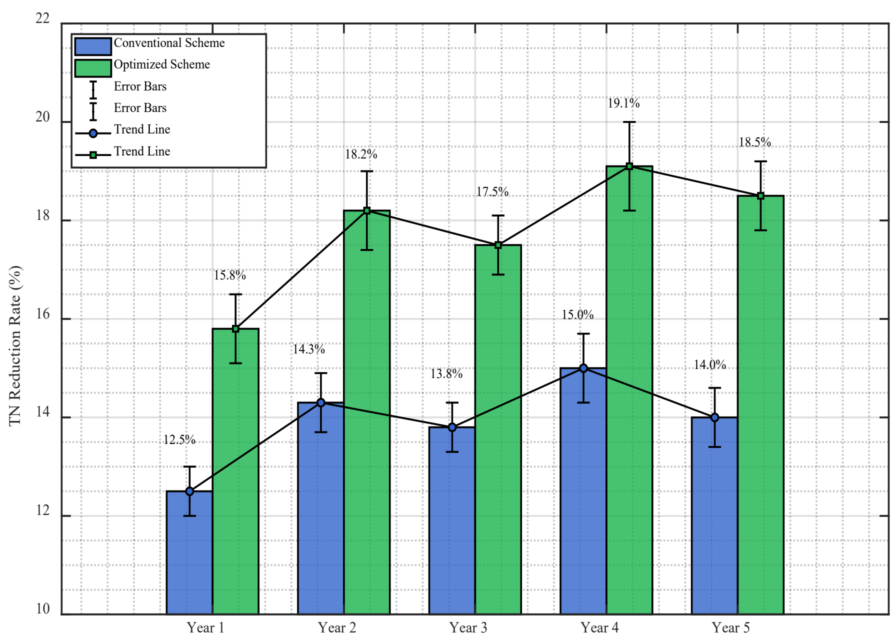

Fig. 3. Total Nitrogen (TN) Load Reduction Rate

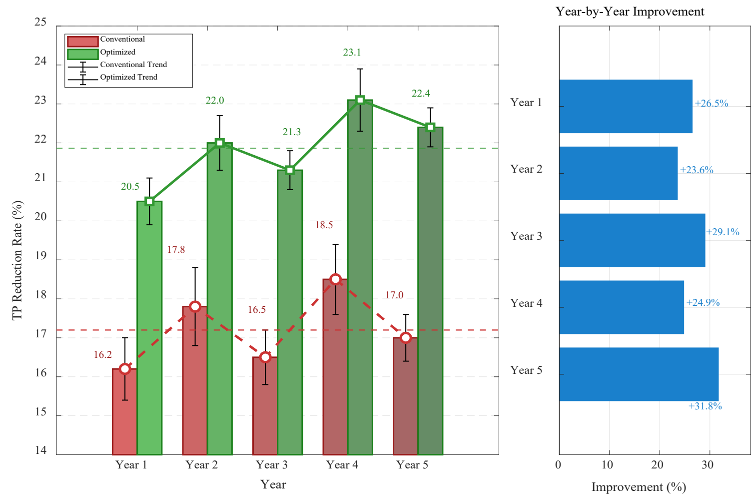

Fig. 4. Total Phosphorus (TP) Load Reduction Rate

The TP reduction rate of the collaborative optimization scheme is also comprehensively leading, with values ranging from 20.5% to 23.1%, significantly higher than the traditional scheme's 16.2% to 18.5%. The collaborative optimization scheme for stable and efficient removal of TP further confirms its design superiority for phosphorus migration characteristics (easy adsorption, easy precipitation). By deploying wetlands and strengthening buffer zones at key nodes of the multi-level ditch system, the retention time of runoff has been effectively extended and the contact surface of the medium has been increased, thereby significantly improving the interception and fixation efficiency of particulate and dissolved phosphorus. This provides a precise and efficient engineering technology paradigm for eutrophication control of water bodies with phosphorus control as the key objective.

Compared with traditional homogenization schemes, the multi-scale collaborative optimization layout scheme can more effectively improve the load reduction rate of TN and TP at the outlet of the watershed. The optimization plan not only improves the average reduction efficiency but also enhances the robustness of the system to cope with interannual hydrological fluctuations by accurately targeting key pollution source areas and migration paths. This proves that optimization design based on spatial heterogeneity analysis and multi-scale coupling has significant advantages in achieving efficient and robust governance of agricultural non-point source pollution.

Carbon Footprint Assessment

In response to the environmental impact assessment of blue-green infrastructure layout schemes, this study systematically conducted a full lifecycle carbon footprint accounting.

By constructing a carbon emission accounting framework that includes four stages of building material production, on-site construction, operation and maintenance, and demolition and recycling, and integrating vegetation system carbon sink benefit calculation, a comparative analysis was conducted between the traditional uniform layout and multi-scale collaborative optimization layout schemes, as shown in Figure 5:

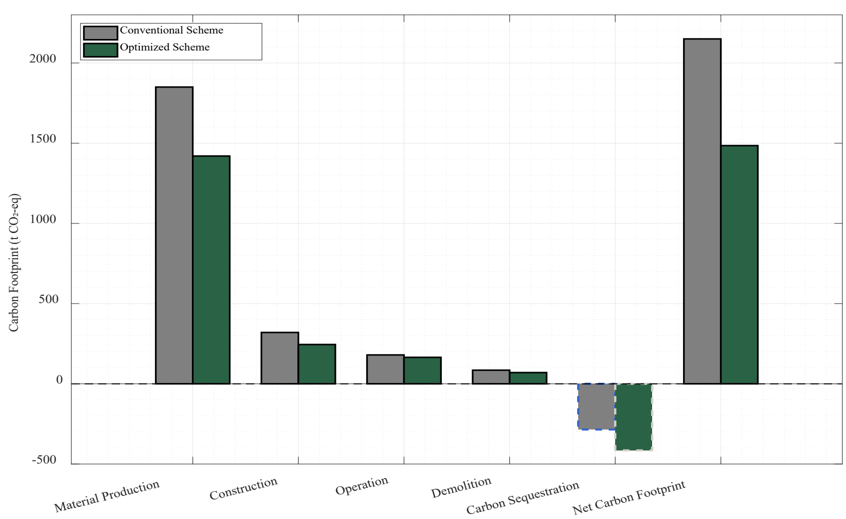

Fig. 5. Life Cycle Carbon Footprint of the Case

The carbon footprint of collaborative optimization schemes at all stages of the lifecycle is significantly lower than that of traditional schemes. The carbon emissions during the production stage of building materials were reduced by 430 tons of CO_2-eq, a decrease of 23.2%. This is mainly attributed to the optimization plan that reduced the total facility area through precise layout, thereby reducing the amount of high carbon emission building materials such as concrete and steel. During the construction phase, carbon emissions were reduced by 75 tons of CO_2-eq, reflecting a decrease in earthwork volume and mechanical operation intensity. Although the differences were minor during the operation and maintenance phases, the optimized scheme still demonstrated higher energy efficiency. Carbon sequestration benefits increased from -285 t CO_2-eq to -415 t CO_2-eq, due to the optimized scheme enhancing the biomass carbon sequestration capacity of wetland vegetation and buffer zone shrubs. The overall net carbon footprint decreased by 665 t CO_2-eq, confirming that multi-scale synergistic optimization can effectively achieve synergistic effects between pollution control and carbon emission reduction.

Conclusion

This study developed an integrated framework combining SWAT-based watershed simulation, NSGA-II multi-objective optimization, and life-cycle assessment to improve the spatial configuration of blue–green infrastructure in an intensive agricultural watershed. The optimized configurations reduced total nitrogen and total phosphorus loads by 15.8%–19.1% and 20.5%–23.1%, respectively, while maintaining a comparatively low net carbon footprint and balancing implementation costs. These findings demonstrate that coordinated interventions across fields, drainage ditches, wetlands, riparian corridors, and rivers can provide greater environmental benefits than isolated pollution-control measures.

By improving water quality and strengthening wetland and riparian connectivity, optimized blue–green infrastructure may reduce major pressures on amphibian breeding, larval-development, foraging, and dispersal habitats. However, water-quality improvement alone cannot confirm positive population-level outcomes. Future studies should incorporate field observations of amphibian abundance, reproductive success, species-specific habitat suitability, hydroperiod requirements, pesticide exposure, and long-term population responses. Overall, this framework provides a practical approach for integrating agricultural pollution mitigation, low-carbon watershed management, and amphibian habitat conservation within a unified planning process.

Acknowledgment.—This work was supported by the Youth Innovation Team of Shaanxi University (2022).

Literature Cited

Ariyarathna IS, Abeyrathna WP, Jamei E, Chau H-W. 2023. A review of the application of blue–green infrastructure (BGI) as an effective urban flood mitigation strategy for livable and healthy cities in Australia. *Architecture 3*(3): 461-476.

Breulmann M, Müller RA, van Afferden M. 2024. Modelling urban stormwater and irrigation management with coupled blue-green infrastructure in the context of climate change. *Blue-Green Systems 6*(1): 100-113.

Guo S, Wang S, Wang Q, Luo Y. 2024. Spatiotemporal Response and Risk Classification of Multifunctional Blue-Green Infrastructure to Landscape Pattern: A Case Study of Sichuan Tianfu New Area. *Journal of Northwest Forestry University 39*(2): 237-292.

Hamel P, Tan L. 2022. Blue–green infrastructure for flood and water quality management in Southeast Asia: evidence and knowledge gaps. *Environmental management 69*(4): 699-718.

Konstantinova A, Filyushkina A, Maximova O, Kerdivar K, Gromova A, Matasov V, Vasenev V. 2024. Uptake of ecosystem service concept in urban blue-green infrastructure planning and decision-making in Russia. *Blue-Green Systems 6*(2): 327-344.

Krivtsov V. 2025. Green and blue-green infrastructure–benefits, trade-offs, and optimisation of ecosystem services: an overview with perspectives for research and management. *Plant Ecology & Diversity 18*(5-6): 267-285.

LIU S, BAI Z, LIU D, SHEN P. 2025. Research Progress in and Planning Strategies for Multi-scale Measurement of the Efficiency of Urban Blue-Green Infrastructure in Carbon Sink Enhancement and Emission Reduction. *Landscape Architecture 32*(1): 14-22.

Mueca CCA, Robles MEL, Uy MJF, Haque MT. 2025. Sustainable Urban Development using Blue-Green Infrastructure: A Review of Flood Mitigation, Heat Reduction, and Water Quality Enhancement. *Journal of Wetlands Research 27*(2): 231-242.

Mugume SN, Nakyanzi LP. 2024. Evaluation of effectiveness of Blue-Green Infrastructure for reduction of pluvial flooding under climate change and internal system failure conditions. *Blue-Green Systems 6*(2): 264-292.

O'Donnell EC, Gosling SN, Netusil NR, Chan FS, Dolman NJ. 2021. Perceptions of blue-green and grey infrastructure as climate change adaptation strategies for urban water resilience. *Journal of the British Academy 9*(s9): 143-182.

Peters H, Landström C. 2022. The public and its assets: Performing appraisal and advocacy for blue and green infrastructure in London, England. *Environment and Planning E: Nature and Space 5*(4): 2193-2215.

Plunge S, Gudas M, Povilaitis A, Piniewski M. 2023. Evaluation of the costs of agricultural diffuse water pollution abatement in the context of Lithuania's water protection goals and climate change. *Environmental management 71*(4): 755-772.

Rojas-Rodríguez IS, Salazar-Solano V, Moreno-Dena JM. 2021. Simulation of agricultural diffuse pollution in the Lower Basin of the Río Mayo. *Agronomía Costarricense 45*(1): 143-151.

Sadegh Koohestani S, Mukheibir P, Wakefield-Rann R, Santamouris M. 2025. Adopting a socio-technical perspective on the challenges and barriers in transitioning to Blue-Green Infrastructure (BGI). *Blue-Green Systems 7*(1): 79-94.

Simeonova T. 2024. Diffuse pollution sources of groundwater in an intensive agricultural area in southern Bulgaria. *Bulgarian Journal of Crop Science 61*(1): 59-67.

Tanık A, Hanedar A, Girgin E, Güneş E, Görgün E, Karakaya N, Gökdereli G, Çankaya BF, Kimence T, Karaaslan Y. 2021. Setting Measures for Tackling Agricultural Diffuse Pollution of Küçük Menderes Basin. *Turkish Journal of Water Science and Management 5*(2): 148-177.

Tanner CC, Tomer MD, Goeller BC. 2025. A framework for applying interceptive mitigations for diffuse agricultural pollution. *New Zealand Journal of Agricultural Research 68*(2): 390-411.

Vetter T. 2022. Co-producing better land management? An ethnographic study of partnership working in the context of agricultural diffuse pollution: Co-producing better land management? An ethnographic study of partnership working in the context of agricultural diffuse pollution. *Review of Agricultural, Food and Environmental Studies 103*(2): 117-141.

Willems JJ, Kenyon AV, Sharp L, Molenveld A. 2021. How actors are (dis) integrating policy agendas for multi-functional blue and green infrastructure projects on the ground. *Journal of environmental policy & planning 23*(1): 84-96.

Willems JJ, Kuitert L, Van Buuren A. 2023. Policy integration in urban living labs: Delivering multi-functional blue-green infrastructure in Antwerp, Dordrecht, and Gothenburg. *Environmental Policy and Governance 33*(3): 258-271.

Winker M, Deffner J, Rohrbach M, Schramm E, Stein M. 2022. Enhancing blue-green infrastructure in German cities with the involvement of urban society: Insights from Frankfurt/Main and Stuttgart. *Blue-Green Systems 4*(2): 230-246.

Yan Q, Zhang A, Yin Y. 2025. Research on the Construction of Water Ecological Security Pattern Based on Blue-Green Infrastructure—Taking Anyang City as an Example. *China Resource Comprehensive Utilization 43*(2): 210-213.

Yonegura VB. 2025. The Presence of Blue Infrastructure in the Interaction between Green Infrastructure and Urban and Regional Planning. *Revista Percurso 17*(1): 295-320.